

On the relationship between the local tracking procedures and monotonic schemes in quantum optimal control

Julien Salomon^{a)}

Laboratoire Jacques-Louis Lions, Université Pierre et Marie Curie, Boîte courrier 187,
75252 Paris Cedex 05, France

Gabriel Turinici^{b)}

CEREMADE, Université Paris Dauphine, Pl. du Maréchal de Lattre de Tassigny,
75755 Paris Cedex 16, France

(Received 2 August 2005; accepted 5 January 2006; published online 16 February 2006)

Numerical simulations of (bilinear) quantum control often rely on either monotonically convergent algorithms or tracking schemes. However, despite their mathematical simplicity, very limited intuitive understanding exists at this time to explain the former type of algorithms. Departing from the usual mathematical formalization, we present in this paper an interpretation of the monotonic algorithms as finite horizon, local in time, tracking schemes. Our purpose is not to present a new class of procedures but rather to introduce the necessary rigorous framework that supports this interpretation. As a by-product we show that at each instant, estimates of the future quality of the current control field are available and used in the optimization. When the target is expressed as reaching a prescribed final state, we also present an intuitive geometrical interpretation as the minimization of the distance between two correlated trajectories: one starting from the given initial state and the other backward in time from the target state. As an illustration, a stochastic monotonic algorithm is introduced. Numerical discretizations of the two procedures are also presented. © 2006 American Institute of Physics. [DOI: [10.1063/1.2170085](https://doi.org/10.1063/1.2170085)]

I. INTRODUCTION

Laser control of complex molecular and solid-state systems is becoming feasible, especially since the introduction¹ of closed-loop laboratory learning techniques and their successful implementation.^{2–6} Accompanying these advances, the computer simulations have the advantage to overcome experimental restrictions and have access to the whole dynamics, allowing further insight and also providing hints in devising future experiments. Many algorithms have been proposed to solve the ensuing optimization problem, among which two distinct classes can be identified. The first one contains the local tracking methods^{7–12} that propose explicit formula of the driving field in an open-loop dependence on the evolving state. The formula is obtained from the requirement to decrease a certain functional defined at each time instant and related to the “distance” to the target or by demanding strict adherence to a predefined observable trajectory. The second class contains the monotonic algorithms^{13–15} that solve the Euler-Lagrange equations associated with the optimization of a quality functional defined at a final time T . The two classes can also be combined as in Ref. 12.

Whereas the local tracking methods enable a very concrete geometric interpretation, the monotonic schemes are only designed by algebraic manipulations, which make their understanding difficult. Building on striking similarities between the two methods, we present in this paper an intuitive

understanding of the operation of the monotonic algorithms. We show that these can be viewed as finite horizon local tracking procedures that ensure the convenient behavior of a time-dependent index encoding the distance to the target. We can go even further demonstrating that at each instant the algorithm is aware, when the target enters linearly, of the *future quality* (i.e., at the *final time T*) of the current driving field. The monotonic algorithms use this value to optimize locally in time. When the target enters quadratically, only a lower bound of the quality index (functional) is available and powerlike methods are used to iterate on the nonlinearity.

Further intuitive interpretation is given when the goal is to reach a prescribed final state. We show that minimization, with respect to the control field, operates on the distance between two important trajectories: the *direct* that starts from the given initial state and the *reference* backward in time from the target state.

We want to emphasize that the algorithms which are presented here—either tracking procedures or monotonic schemes—are not new and are not to be considered as innovative. We do try instead to give an intuitive meaning of the monotonic schemes. Indeed, as far as we know, no concrete interpretation of this class of algorithms has ever been presented and the only base of these algorithms consists in a technical computation, where the algebraic manipulations do not illuminate the concrete meaning of the result. This lack of comprehension makes the monotonic schemes difficult to analyze, improve, or combine with other optimization proce-

^{a)}Electronic mail: salomon@ann.jussieu.fr

^{b)}Electronic mail: gabriel.turinici@dauphine.fr

dures. To illustrate the prospects that our work allows to consider, we introduce a stochastic monotonic algorithm that makes early use of the information available through the *forward quality functional*.

The paper is balanced as follows. The necessary background on tracking procedures is presented in Sec. II. Then, in Sec. III we develop our theory for the density-matrix formulation, followed in Sec. IV by that for wave functions. The stochastic monotonic algorithm is introduced in Sec. V. We then illustrate our results with a numerical simulation in Sec. VI. Finally, we present concluding remarks in Sec. VII.

II. TRACKING PROCEDURES

Consider a state variable $x(t)$ driven by a control $u(t)$ according to the equation

$$\frac{dx(t)}{dt} = (A + u(t)B)x(t). \quad (1)$$

The tracking approach consists in introducing a *tracking index* $\check{y}(t) = y(\int_0^t u^2(s)ds, x(t))$ measuring the quality of the control u ; this index is required to increase through an appropriate choice of u . In order to design u , one may compute the derivative of $\check{y}(t)$,

$$\frac{d\check{y}(t)}{dt} = D_1 yu(t) + D_2 y(A + u(t)B)x(t),$$

where D_j is the partial derivative with respect to the j th variable. This can be further expressed as

$$\frac{d\check{y}(t)}{dt} = f(F(t), x(t)) + u(t)g(F(t), x(t)), \quad (2)$$

where $F(t) = \int_0^t u^2(s)ds$. It is seen that, except for the points where g vanishes (which will be called singularities and will be treated separately) for any desired trajectory \tilde{y} with $\tilde{y}(0) = y_0$, the condition $\check{y}(t) = \tilde{y}(t)$ uniquely determines the field $u(t)$ by the formula

$$u(t) = \frac{[d\tilde{y}(t)/dt] - f(F(t), x(t))}{g(F(t), x(t))}. \quad (3)$$

From $dF/dt = u^2(t)$ one obtains that (3) is, in fact, an ordinary differential equation (ODE) on F of the form

$$dF/dt = \mathcal{Y}(F, x) \quad (4)$$

that is to be solved jointly with (1) in order to ensure adherence to the prescribed trajectory \tilde{y} .

Same considerations apply if only weaker properties are required, typically the increase/decrease of $\check{y}(t)$ which can be enforced through the *tracking condition* $[d\check{y}(t)/dt] \geq 0$ (≤ 0). The difficulty of this approach is to find a suitable reference tracking trajectory \tilde{y} that does not encounter singular points of the systems (2) and (4), i.e., where $g(F, x) = 0$. In general singular points cannot be avoided beforehand and techniques were designed to treat such situations: see Ref. 10 for designs that locally alter the trajectory to circumvent the singular points and Refs. 12 and 16 for a study of the stopping points and procedures to improve their optimality.

III. DENSITY-MATRIX FORMULATION

Consider a quantum system with internal dynamics described by the Hamiltonian H_0 . Its interaction with an external field is modeled by introducing the time-independent dipole moment operator μ and the field intensity $\varepsilon(t)$. If the system is represented in the density-matrix formulation with initial state ρ_0 , its dynamics will obey the time-dependent Schrödinger equations

$$\begin{aligned} i\frac{\partial}{\partial t}\rho(x, t) &= [H_0 - \varepsilon(t)\mu, \rho(x, t)], \\ \rho(x, t=0) &= \rho_0(x), \end{aligned} \quad (5)$$

where x denotes the relevant spatial coordinates and $[., .]$ the commutator of two operators. We used the convention $\hbar=1$. We introduce the Liouville space representation, by defining the scalar product $\langle\langle a, b \rangle\rangle = \text{Tr}(a^\dagger b)$, where a^\dagger denotes the adjoint of the matrix a , and the associated norm $\|a\|_\gg = \sqrt{\langle\langle a, a \rangle\rangle}$. Instead of the commutators above, we define the linear operators \mathcal{H} and \mathcal{M} that act on the density matrices as $\mathcal{H}\rho = [H_0, \rho]$ and $\mathcal{M}\rho = [\mu, \rho]$. Equation (5) becomes

$$\begin{aligned} i\frac{\partial}{\partial t}\rho(x, t) &= (\mathcal{H} - \varepsilon(t)\mathcal{M})\rho(x, t), \\ \rho(x, t=0) &= \rho_0(x), \end{aligned} \quad (6)$$

with $t \in [0, T]$. The control goal can be expressed through the introduction of an observable operator O by the requirement that the quantity $\Re\langle\langle O, \rho(T) \rangle\rangle$ be maximized (\Re denotes the real part of a complex number). The corresponding quality functional to be maximized can be defined by

$$J(\varepsilon) = 2\Re\langle\langle O, \rho(T) \rangle\rangle - \int_0^T \alpha\varepsilon^2(t)dt. \quad (7)$$

A. Tracking algorithm

The methodology described in Sec. II does not specify any particular time of control. However, several problems consider a bounded total control time, e.g., when maximizing J . In order to tackle such a problem, consider the backward trajectory $\rho_{\text{ref}}(t)$ defined by

$$\begin{aligned} i\frac{\partial}{\partial t}\rho_{\text{ref}}(x, t) &= (\mathcal{H} - \tilde{\varepsilon}(t)\mathcal{M})\rho_{\text{ref}}(x, t), \\ \rho_{\text{ref}}(x, t=T) &= O, \end{aligned} \quad (8)$$

where $\tilde{\varepsilon}$ is a given field.

Let us denote by $\varepsilon_{\varepsilon, \tilde{\varepsilon}, t}$ the field obtained by taking $\varepsilon(s)$ up to t and $\tilde{\varepsilon}(s)$ afterward,

$$\varepsilon_{\varepsilon, \tilde{\varepsilon}, t}(s) = \begin{cases} \varepsilon(s), & 0 \leq s \leq t \\ \tilde{\varepsilon}(s), & t < s \leq T. \end{cases} \quad (9)$$

If $\varepsilon(s)$ is only known up to a time $t \in [0, T]$, a natural candidate for the control field is $\varepsilon_{\varepsilon, \tilde{\varepsilon}, t}$. Since $\Re\langle\langle \rho_{\text{ref}}(t), \rho(t) \rangle\rangle = \Re\langle\langle \rho_{\text{ref}}(T), \rho(T) \rangle\rangle$, its functional value $J(\varepsilon_{\varepsilon, \tilde{\varepsilon}, t})$ is $2\Re\langle\langle \rho_{\text{ref}}(t), \rho(t) \rangle\rangle - \int_0^t \alpha\varepsilon^2(s)ds - \int_t^T \alpha\tilde{\varepsilon}^2(s)ds$. Let us introduce

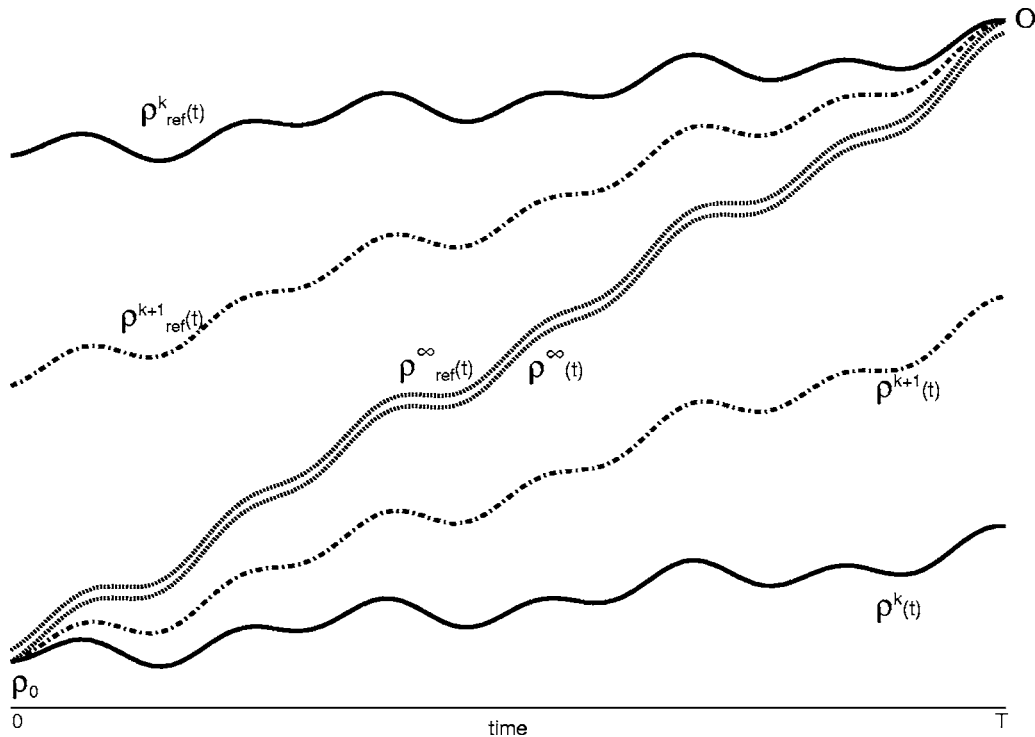


FIG. 1. Schematic illustration of the convergence of the monotonic algorithms for negligible fluence. The evolving state ρ^{k+1} is approaching monotonically the reference trajectory ρ_{ref}^k . Without any optimization during the backward propagation (i.e., choosing $\tilde{\varepsilon}^{k+1} = \varepsilon^{k+1}$), at the next iteration, ρ_{ref}^{k+1} will remain at a constant distance from ρ^{k+1} because both use the same field ε^{k+1} . This shrinking distance between the two trajectories ensures the progression of the quality functional toward optimal values. This observation is currently used in the context of efficient parallelization of the numerical resolution of quantum control problems (Ref. 17). In the general case, the decreasing character of the distance between the curves is weighted by the field fluence and the optimal couple of trajectories will be a tube whose nonzero width is related to the driving laser field fluence.

the tracking index $J_{\varepsilon, \tilde{\varepsilon}}^{\text{fwd}}$ to be maximized, called in this case forward quality functional,

$$J_{\varepsilon, \tilde{\varepsilon}}^{\text{fwd}}(t) = 2\Re\langle\langle \rho_{\text{ref}}(t), \rho(t) \rangle\rangle - \int_0^t \alpha \varepsilon^2(s) ds - \int_t^T \alpha \tilde{\varepsilon}^2(s) ds. \quad (10)$$

Note that if the field ε drives ρ from $\rho(0) = \rho_0$ to $\rho(T) = O$ then $\tilde{\varepsilon} = \varepsilon$ drives ρ_{ref} from $\rho_{\text{ref}}(T) = O$ to $\rho_{\text{ref}}(0) = \rho_0$. Following this remark, an adaptation of the local tracking approach consists in recursively computing a backward propagation (8) with $\tilde{\varepsilon} = \tilde{\varepsilon}^k$ followed by a forward propagation by (6) with $\varepsilon = \varepsilon^{k+1}$ while ensuring that the forward quality functional increases in time for the forward propagation and increases in reverse time for the backward propagation. We obtain the tracking conditions

$$\frac{d}{dt} J_{\varepsilon^k, \tilde{\varepsilon}^k}^{\text{fwd}}(t) \leq 0 \quad (11)$$

and

$$\frac{d}{dt} J_{\varepsilon^{k+1}, \tilde{\varepsilon}^k}^{\text{fwd}}(t) \geq 0. \quad (12)$$

A computation similar to the one in (2) shows that the monotonicities (11) and (12) are equivalent to

$$(\tilde{\varepsilon}^k(t) - \varepsilon^k(t))(2\Im\langle\langle \rho_{\text{ref}}^k(t), \mathcal{M}\rho^k(t) \rangle\rangle + \alpha(\varepsilon^k(t) + \tilde{\varepsilon}^k(t))) \leq 0 \quad (13)$$

and

$$(\tilde{\varepsilon}^k(t) - \varepsilon^{k+1}(t))(2\Im\langle\langle \rho_{\text{ref}}^k(t), \mathcal{M}\rho^{k+1}(t) \rangle\rangle + \alpha(\varepsilon^{k+1}(t) + \tilde{\varepsilon}^k(t))) \geq 0, \quad (14)$$

where \Im denotes the imaginary part of a complex number. These inequalities are the tracking conditions corresponding to the forward quality functional $J_{\varepsilon, \tilde{\varepsilon}}^{\text{fwd}}$. It is important to note that

$$J_{\varepsilon, \tilde{\varepsilon}}^{\text{fwd}} = \|O\|_{\gg}^2 + \|\rho_0\|_{\gg}^2 - \|\rho^k(t) - \rho_{\text{ref}}^k(t)\|_{\gg}^2 - \int_0^t \alpha \varepsilon^2(s) ds - \int_t^T \alpha \tilde{\varepsilon}^2(s) ds. \quad (15)$$

The procedure above suggests the following interpretation. For any candidate solution ε^k two trajectories can be computed: $\rho^k(t)$ that starts from the correct initial condition ρ_0 but whose final state $\rho^k(T)$ may not yet be satisfactory close to the matrix O , and the state $\rho_{\text{ref}}^k(t)$ that propagates backward from the matrix O but may not reach the correct initial state ρ_0 ; the idea is to diminish the intertrajectory distance by computing ε^{k+1} such that $\rho^{k+1}(t)$ approaches monotonically $\rho_{\text{ref}}^k(t)$ and vice versa. In the approximation where the fluence penalty $\alpha \int_0^T \varepsilon^2(t) dt$ is negligible before the control part $\|\rho^k(t) - \rho_{\text{ref}}^k(t)\|_{\gg}$ the distance between the two trajectories will de-

crease during the propagation. The next propagation carries on this process further and so on. The situation is schematically depicted in Fig. 1.

We are now in position to claim the following result.

Theorem 1. Suppose that the sequences $(\tilde{\varepsilon}^k(t))_{k \in \mathbb{N}}$ and $(\varepsilon^k(t))_{k \in \mathbb{N}}$ fulfill the tracking conditions (11) and (12). These sequences optimize monotonically the quality functional J in the sense that

$$J(\varepsilon^k) \leq J(\varepsilon^{k+1}). \quad (16)$$

Moreover

$$\begin{aligned} J(\varepsilon_{\varepsilon^k, \tilde{\varepsilon}^k, t_0}) &\leq J(\varepsilon_{\varepsilon^k, \tilde{\varepsilon}^k, t_0}), \quad J(\varepsilon_{\varepsilon^{k+1}, \tilde{\varepsilon}^k, t_0}) \leq J(\varepsilon_{\varepsilon^{k+1}, \tilde{\varepsilon}^k, t_0}), \\ 0 \leq t_0 \leq t'_0 &\leq T. \end{aligned} \quad (17)$$

Proof. A simple computation shows that

$$\begin{aligned} J(\varepsilon_{\varepsilon^k, \tilde{\varepsilon}^k, t_0}) - J(\varepsilon_{\varepsilon^k, \tilde{\varepsilon}^k, t_0}) \\ = \int_{t_0}^{t'_0} (\tilde{\varepsilon}^k(s) - \varepsilon^k(s))(2\Im\langle\langle \rho_{\text{ref}}^k(s), \mathcal{M}\rho^k(s) \rangle\rangle \\ + \alpha(\varepsilon^k(s) + \tilde{\varepsilon}^k(s)))ds \end{aligned} \quad (18)$$

and

$$\begin{aligned} J(\varepsilon_{\varepsilon^{k+1}, \tilde{\varepsilon}^k, t_0}) - J(\varepsilon_{\varepsilon^{k+1}, \tilde{\varepsilon}^k, t_0}) \\ = \int_{t_0}^{t'_0} (\tilde{\varepsilon}^k(s) - \varepsilon^{k+1}(s))(2\Im\langle\langle \rho_{\text{ref}}^k(s), \mathcal{M}\rho^{k+1}(s) \rangle\rangle \\ + \alpha(\varepsilon^{k+1}(s) + \tilde{\varepsilon}^k(s)))ds, \end{aligned} \quad (19)$$

which are positive quantities, since the tracking conditions (11) and (12) are fulfilled; we thus obtained (17). Monotonicity (16) is a simple consequence,

$$J(\varepsilon^k) = J(\varepsilon_{\varepsilon^k, \tilde{\varepsilon}^k, T}) \leq J(\varepsilon_{\varepsilon^{k+1}, \tilde{\varepsilon}^k, T}) = J(\varepsilon^{k+1}). \quad (20)$$

Note that (18) and (19) also prove that for any intermediary time $t < T$ the quality functional will take the value $J_{\varepsilon^k, \tilde{\varepsilon}^k}^{\text{fwd}}(t)$ [respectively, $J_{\varepsilon^{k+1}, \tilde{\varepsilon}^k}^{\text{fwd}}(t)$] if the optimization is stopped at the instant $t \leq T$ during the backward (respectively, forward) propagation. The value of $J_{\varepsilon, \tilde{\varepsilon}}^{\text{fwd}}(t)$ is readily computed at any time t as soon as the backward propagation (8) is computed. Armed with this tool, optimization need not wait till the final time (T) but can instead already operate at the current time (t) using local tracking procedures to optimize the value $J_{\varepsilon, \tilde{\varepsilon}}^{\text{fwd}}(t)$.

This particular observation can be framed into the more general approach of *model predictive control*^{18–20} (MPC) that aims to improve the standard feedback control by predicting how a system will react to controls allowing to optimize the *future behavior* of a plant. This prediction operates through the introduction of an empirical model that describes the system. Two particularities are to be observed to fully compare our approach with MPC: firstly, we operate in regimes very far from equilibrium or any perturbative approximation, while MPC works better as stabilizer; secondly, in quantum control, the future quality of a particular control is obtained at *no additional cost* as algebraic manipulations on the numerical data are already available. This latter fact of crucial

importance enables us to see the monotonic algorithms as a MPC of the simulated model, at the crossroad between tracking and iterative optimal control.

B. Monotonic schemes as local tracking procedures

In an approach different from tracking, monotonically convergent algorithms, pioneered in Refs. 21 and 22 and extended in Ref. 15 in the wave-function representation, are used in the context of the density-matrix operator as in Refs. 23 and 24. These schemes seek the critical points of $J(\varepsilon)$ under the constraint of satisfying (6). Because of the constraint, a Lagrange multiplier, denoted as $\rho_{\text{ref}}(x, t)$ (for reasons that will be made clear latter), is introduced in the quality functional that now reads as

$$\begin{aligned} J(\varepsilon) = 2\Re\langle\langle O, \rho(T) \rangle\rangle - \int_0^T \alpha\varepsilon^2(s)ds \\ - 2\Re \left\{ \int_0^T \left\| \rho_{\text{ref}}, \frac{\partial \rho(s)}{\partial t}(s) \right. \right. \\ \left. \left. - \frac{(\mathcal{H} - \varepsilon(s)\mathcal{M})\rho(s)}{i} \right\| ds \right\}. \end{aligned} \quad (21)$$

The critical-point equations read as

$$\begin{aligned} i\frac{\partial}{\partial t}\rho(x, t) &= (\mathcal{H} - \varepsilon(t)\mathcal{M})\rho(x, t), \\ \rho(x, t=0) &= \rho_0(x), \\ \alpha\varepsilon(t) + \Im\langle\langle \rho_{\text{ref}}(t), \mathcal{M}\rho(t) \rangle\rangle &= 0, \\ i\frac{\partial}{\partial t}\rho_{\text{ref}}(x, t) &= (\mathcal{H} - \varepsilon(t)\mathcal{M})\rho_{\text{ref}}(x, t), \\ \rho_{\text{ref}}(x, T) &= O. \end{aligned} \quad (22)$$

Note that the Lagrange multiplier ρ_{ref} fulfills the same equations as the state ρ_{ref} defined in Eq. (8) (hence our notations). Building on these relations, the *monotonic algorithms* prescribe a particular order to iterate in these coupled equations by constructing, at the iteration step $k \rightarrow k+1$, a field $\varepsilon^{k+1}(t)$ with the important property (16), hence the name of monotonic algorithm. An example of such algorithm is²⁴

$$\begin{aligned} i\frac{\partial}{\partial t}\rho_{\text{ref}}^k(x, t) &= (\mathcal{H} - \varepsilon^k(t)\mathcal{M})\rho_{\text{ref}}^k(x, t), \\ \rho_{\text{ref}}^k(x, T) &= O, \\ \varepsilon^k(t) &= (1 - \eta)\varepsilon^k(t) - \frac{\eta}{\alpha}\Im\langle\langle \rho_{\text{ref}}^k(t), \mathcal{M}\rho^k(t) \rangle\rangle, \\ i\frac{\partial}{\partial t}\rho^{k+1}(x, t) &= (\mathcal{H} - \varepsilon^{k+1}(t)\mathcal{M})\rho^{k+1}(x, t), \\ \rho^{k+1}(x, t=0) &= \rho_0(x), \end{aligned} \quad (23)$$

$$\varepsilon^{k+1}(t) = (1 - \delta)\tilde{\varepsilon}^k(t) - \frac{\delta}{\alpha} \Im \langle \langle \rho_{\text{ref}}^k(t), \mathcal{M} \rho^{k+1}(t) \rangle \rangle. \quad (24)$$

The following theorem specifies the link between this scheme and a local tracking procedure.

Theorem 2. The sequences $(\varepsilon^k)_{k \in \mathbb{N}}$ and $(\tilde{\varepsilon}^k)_{k \in \mathbb{N}}$ defined by (23) and (24) fulfill the tracking conditions (11) and (12). In particular, monotonicity (16) follows from Theorem 1.

Proof. Replacing scalar products in (13) and (14) via (23) and (24), we obtain

$$\begin{aligned} & (\tilde{\varepsilon}^k(t) - \varepsilon^k(t))(2\Im \langle \langle \rho_{\text{ref}}^k(t), \mathcal{M} \rho^k(t) \rangle \rangle + \alpha(\varepsilon^k(t) + \tilde{\varepsilon}^k(t))) \\ &= -\left(\frac{2}{\eta} - 1\right)(\varepsilon^k(t) - \tilde{\varepsilon}^k(t))^2, \end{aligned} \quad (25)$$

$$\begin{aligned} & (\tilde{\varepsilon}^k(t) - \varepsilon^{k+1}(t))(2\Im \langle \langle \rho_{\text{ref}}^k(t), \mathcal{M} \rho^{k+1}(t) \rangle \rangle + \alpha(\varepsilon^{k+1}(t) \\ &+ \tilde{\varepsilon}^k(t))) = \left(\frac{2}{\delta} - 1\right)(\varepsilon^{k+1}(t) - \tilde{\varepsilon}^k(t))^2, \end{aligned} \quad (26)$$

and (11) and (12) follows.

IV. WAVE-FUNCTION FORMULATION

Consider a quantum system with internal Hamiltonian H_0 prepared in the initial state $\psi_0(x)$. In the presence of an external interaction, the new Hamiltonian is $H = H_0 - \varepsilon(t)\mu$ the state $\psi(x, t)$ at time t satisfies the time-dependent Schrödinger equations to be controlled,

$$\begin{aligned} i \frac{\partial}{\partial t} \psi(x, t) &= (H_0 - \varepsilon(t)\mu) \psi(x, t), \\ \psi(x, t=0) &= \psi_0(x). \end{aligned} \quad (27)$$

The control goal can be expressed through the introduction of either a target wave function or an observable operator O , by the requirement that the corresponding quantities $2\Re \langle \psi_{\text{target}} | \psi(T) \rangle$ or $\langle \psi(T) | O | \psi(T) \rangle$ be maximized. Two examples of quality functionals corresponding to these goals can be defined by

$$J_1(\varepsilon) = 2\Re \langle \psi_{\text{target}} | \psi(T) \rangle - \int_0^T \alpha \varepsilon^2(s) ds, \quad (28)$$

$$J_2(\varepsilon) = \langle \psi(T) | O | \psi(T) \rangle - \int_0^T \alpha \varepsilon^2(s) ds. \quad (29)$$

Results similar to those of previous sections can be obtained with this formulation.

A. Tracking algorithms for J_1 and J_2

As in Sec. III A, we define a backward trajectory ψ_{ref} from a target wave function ψ_f^k with a field $\tilde{\varepsilon}$,

$$\begin{aligned} i \frac{\partial}{\partial t} \psi_{\text{ref}}(t, x) &= (H_0 - \tilde{\varepsilon}(t)\mu) \psi_{\text{ref}}(t, x), \\ \psi_{\text{ref}}^k(T, x) &= \psi_f^k(x), \end{aligned} \quad (30)$$

where $\psi_f^k(x) = \psi_{\text{target}}(x)$ when J_1 is used and $\psi_f^k(x) = O\psi^k(x, T)$ for J_2 . We introduce the forward quality functional,

$$J_{\varepsilon, \tilde{\varepsilon}}^{\text{fwd}}(t) = 2\Re \langle \psi_{\text{ref}}(t) | \psi(t) \rangle - \int_0^t \alpha \varepsilon^2(s) ds - \int_t^T \alpha \tilde{\varepsilon}^2(s) ds. \quad (31)$$

The monotonic progression of the functionals

$$\frac{d}{dt} J_{\varepsilon^k, \tilde{\varepsilon}^k}^{\text{fwd}}(t) \leq 0 \quad (32)$$

and

$$\frac{d}{dt} J_{\varepsilon^{k+1}, \tilde{\varepsilon}^k}^{\text{fwd}}(t) \geq 0 \quad (33)$$

is equivalent to the corresponding tracking conditions

$$(\tilde{\varepsilon}^k(t) - \varepsilon^k(t))(2\Im \langle \psi_{\text{ref}}^k(t) | \mu | \psi^k(t) \rangle + \alpha(\varepsilon^k(t) + \tilde{\varepsilon}^k(t))) \leq 0 \quad (34)$$

and

$$(\tilde{\varepsilon}^k(t) - \varepsilon^{k+1}(t))(2\Im \langle \psi_{\text{ref}}^k(t) | \mu | \psi^{k+1}(t) \rangle + \alpha(\varepsilon^{k+1}(t) + \tilde{\varepsilon}^k(t))) \geq 0. \quad (35)$$

A theorem similar to the Theorem 1 can be obtained for J_1 .

Theorem 3. Let us define $\varepsilon_{\varepsilon, \tilde{\varepsilon}, t_0}$ by (9) and suppose that the sequences $(\tilde{\varepsilon}^k(t))_{k \in \mathbb{N}}$ and $(\varepsilon^k(t))_{k \in \mathbb{N}}$ fulfill the tracking conditions (32) and (33). Then these sequences optimize monotonically the quality functional J_1 in the sense that

$$J(\varepsilon^k) \leq J(\varepsilon^{k+1}). \quad (36)$$

Moreover

$$\begin{aligned} J(\varepsilon_{\varepsilon^k, \tilde{\varepsilon}^k, t_0}) &\leq J(\varepsilon_{\varepsilon^k, \tilde{\varepsilon}^k, t_0}), \quad J(\varepsilon_{\varepsilon^{k+1}, \tilde{\varepsilon}^k, t_0}) \leq J(\varepsilon_{\varepsilon^{k+1}, \tilde{\varepsilon}^k, t_0}), \\ 0 &\leq t_0 \leq t'_0 \leq T. \end{aligned} \quad (37)$$

The proof is similar to that of Theorem 1.

Remark 1. On the tracking algorithm corresponding to J_2 : A problem embedded into the optimization of J_2 is to maximize $\langle X | O | X \rangle$ subject to $\|X\|=1$. This can be solved using the power method by computing recursively X^k with the formula $X^{k+1} = O(X^k) / \|O(X^k)\|$. Note that when $O \geq 0$ this convergence is monotonic too,

$$\langle X^{k+1} | O | X^{k+1} \rangle \geq \langle X^k | O | X^k \rangle.$$

A way to couple this method with a control problem over $[0, T]$ consists in redefining the target at each iteration of a local tracking procedure by $\psi_{\text{target}}^k = O(\psi^k(T))$. This modification leads to a backward reference trajectory defined at the step k by

$$\begin{aligned} i \frac{\partial}{\partial t} \psi_{\text{ref}}^k(x, t) &= (H_0 - \tilde{\varepsilon}^k(t) \mu) \psi_{\text{ref}}^k(x, t), \\ \psi_{\text{ref}}^k(x, t=T) &= \psi_{\text{target}}^k(x) = O(\psi^k(T)). \end{aligned} \quad (38)$$

The definition of the tracking index (31) is the same. Neglecting control fluence, we are led to maximize $2\Re\langle\psi_{\text{ref}}^k(t)|\psi(t)\rangle$. The optimal value under the constraint $\|\psi(t)\|=1$ is realized for $\psi(t)=O(\psi^k(T))/\|O(\psi^k(T))\|$. Thus, this procedure is an adaptation of the power method. Furthermore, when $O \geq 0$, the monotonicity of the algorithm is preserved at the final time since $J_{\varepsilon^{k+1}, \tilde{\varepsilon}^{k+1}}^{\text{fwd}}(T) - J_{\varepsilon^k, \tilde{\varepsilon}^k}^{\text{fwd}}(T) \geq 0$,

$$\begin{aligned} J(\varepsilon^{k+1}) - J(\varepsilon^k) &= \langle \psi^{k+1}(T) - \psi^k(T) | O | \psi^{k+1}(T) - \psi^k(T) \rangle \\ &\quad + J_{\varepsilon^{k+1}, \tilde{\varepsilon}^k}^{\text{fwd}}(T) - J_{\varepsilon^{k+1}, \tilde{\varepsilon}^k}^{\text{fwd}}(0) + J_{\varepsilon^k, \tilde{\varepsilon}^k}^{\text{fwd}}(0) \\ &\quad - J_{\varepsilon^k, \tilde{\varepsilon}^k}^{\text{fwd}}(T), \end{aligned}$$

which is a sum of positive terms, provided that the tracking conditions (34) and (35) are fulfilled.

B. Monotonic scheme as local tracking procedure

As in Sec. III B, monotonic schemes corresponding to J_1 and J_2 can be defined by

$$\begin{aligned} i \frac{\partial}{\partial t} \psi_{\text{ref}}^k(x, t) &= (H_0 - \tilde{\varepsilon}^k(t) \mu) \psi_{\text{ref}}^k(x, t), \\ \psi_{\text{ref}}^k(x, t=T) &= \psi_f^k(x), \end{aligned} \quad (39)$$

$$\tilde{\varepsilon}^k(t) = (1 - \eta) \varepsilon^k(t) - \frac{\eta}{\alpha} \Im\langle\psi_{\text{ref}}^k(t)|\mu|\psi^k(t)\rangle, \quad (40)$$

$$\begin{aligned} i \frac{\partial}{\partial t} \psi^{k+1}(x, t) &= (H_0 - \varepsilon^{k+1}(t) \mu) \psi^{k+1}(x, t), \\ \psi^{k+1}(x, t=0) &= \psi_0(x), \end{aligned} \quad (41)$$

$$\varepsilon^{k+1}(t) = (1 - \delta) \tilde{\varepsilon}^k(t) - \frac{\delta}{\alpha} \Im\langle\psi_{\text{ref}}^k(t)|\mu|\psi^{k+1}(t)\rangle, \quad (42)$$

where $\psi_f^k(x) = \psi_{\text{target}}^k(x)$ in the case of J_1 and $\psi_f^k(x) = O\psi^k(x, T)$ in the case of J_2 . We have kept the notation ψ_{ref} since its evolution equation (39) is (38). We recognize the Zhu and Rabitz algorithm for $\delta=1$ and $\eta=1$ and the Krotov (as in Tannor *et al.*²²) formulation for $\delta=1$ and $\eta=0$. Note that in the case of J_2 , the algorithm exactly coincides with the tracking algorithm described in remark 1. These algorithms converge monotonically in the sense that $J_i(\varepsilon^{k+1}) \geq J_i(\varepsilon^k)$ for $i=1, 2$.

Although the latter class of schemes covers a large set of monotonic algorithms, it does not represent all these procedures. Further examples are presented in Ref. 25.

A computation similar to the one that had led to Theorem 2 allows to obtain the following.

Theorem 4. The sequences $(\varepsilon^k)_{k \in \mathbb{N}}$ and $(\tilde{\varepsilon}^k)_{k \in \mathbb{N}}$ defined by (41) and (40) fulfill the tracking conditions (32) and (33). In particular, if O is a semipositive-definite observable, the convergence is monotonic in the sense of (36).

Proof. The proof of (32) and (33) is left to the reader. A computation leads to

$$J_1(\varepsilon^{k+1}) - J_1(\varepsilon^k) = \int_0^T -\frac{d}{dt} J_{\varepsilon^k, \tilde{\varepsilon}^k}^{\text{fwd}}(t) + \frac{d}{dt} J_{\varepsilon^{k+1}, \tilde{\varepsilon}^k}^{\text{fwd}}(t) dt, \quad (43)$$

$$\begin{aligned} J_2(\varepsilon^{k+1}) - J_2(\varepsilon^k) &= \langle \psi^{k+1}(T) - \psi^k(T) | O | \psi^{k+1}(T) - \psi^k(T) \rangle \\ &\quad + \int_0^T -\frac{d}{dt} J_{\varepsilon^k, \tilde{\varepsilon}^k}^{\text{fwd}}(t) + \frac{d}{dt} J_{\varepsilon^{k+1}, \tilde{\varepsilon}^k}^{\text{fwd}}(t) dt, \end{aligned} \quad (44)$$

which proves (36).

Remark 2. On the monotonicity condition: The common property of all the monotonic algorithms is that they guarantee to improve at each step the value of a quality functional. However, an attentive study of the proof of the monotonicity of these schemes reveals that all these procedures ensure a stronger condition than the mere monotonicity of quality functional values. This condition relies on the standard formulas (43) and (44). In fact, all monotonic schemes are designed so that each term in the integral is positive, which exactly correspond to the tracking conditions. The identification of the monotonic scheme with a local tracking algorithm is intrinsic, and it exists for most monotonic schemes.

Remark 3. When the quality functional is J_1 , similar considerations as those in Fig. 1 apply: the trajectories of the direct state ψ^k and reference ψ_{ref}^k are at constant distance. This distance is reduced by the choice of ε^{k+1} , and then $\tilde{\varepsilon}^{k+1}$... until convergence to a tube with diameter weighted by the penalization of the field fluence.

V. STOCHASTIC MONOTONIC ALGORITHM

In order to better illuminate the perspectives rendered accessible by our new interpretation of the monotonic algorithms, we introduce a new procedure that uses the forward quality functional in order to optimize the search while solving the Schrödinger equation.

It has been demonstrated¹⁶ that some monotonic algorithms in the density-matrix formulation are slow to achieve convergence or may stop in a local minima. It was seen that the freedom to change the parameters δ and η can bring the required flexibility to circumvent this problem. To improve even further such approaches, we present here the following stochastic monotonic algorithm.

We start from the remark that in the case of a bad convergence, the forward quality functional (10) stagnates while the distance between the forward and backward propagations is still large. An intuitive remedy consists then in detecting when $J_{\varepsilon, \tilde{\varepsilon}}^{\text{fwd}}(t)$ does not sensibly increase any more and then change the parameters δ and η to continue the optimization with a (presumably) more suitable algorithm. In this approach, the forward quality functional plays the role of an indicator allowing to modify online the optimization process. Unlike in Ref. 16 the change of parameters may be decided during the propagation and need not wait the end of the current iteration to be implemented.

Although a coherent procedure to govern the change of the parameters has been documented (see Appendix B of

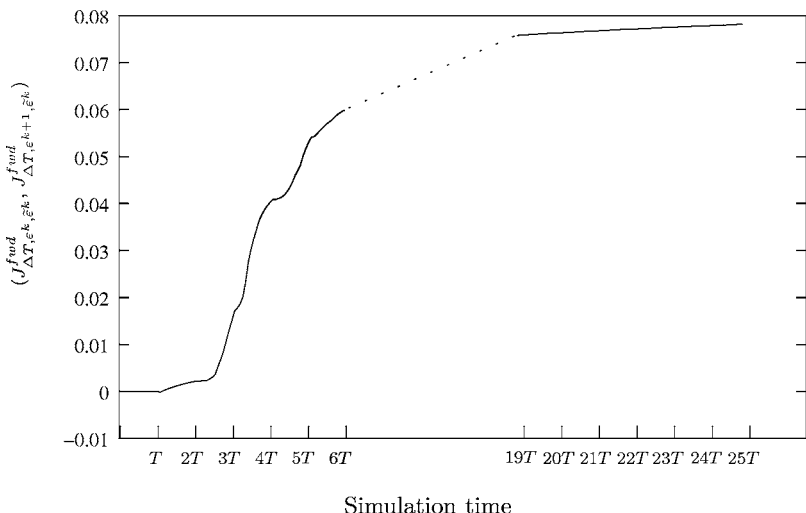


FIG. 2. The optimization procedure gives rise to successive forward and backward propagations. We plot alternatively, for $0 \leq t \leq T$, $J_{\Delta T, \varepsilon^k}^{fwd}(T-t)$ corresponding to the abscissa $t+2kT$ and $J_{\Delta T, \varepsilon^{k+1}}^{fwd}(t)$ corresponding to the abscissa $t+(2k+1)T$. Monotonic increase of the indices all throughout the simulation is observed.

Ref. 16) that acts through the evaluation of a gradient (requiring an additional resolution of the Schrödinger equation), the possibility to *immediately* measure the improvement (if any) allows for an even more practical proposal: at any time step the growing rate of the forward quality functional is computed. If the rate is lower than a given threshold, the parameters δ and η are redefined using a uniform random number generator in $[0,2]$. Note that the parameters δ and η can be changed repeatedly at no additional cost at each time step until satisfactory progression toward the target is obtained.

VI. SIMULATIONS

A. Control of the O–H bond

In order to illustrate the theoretical results, we consider a case already treated in the literature: the O–H bond that vibrates in a Morse-type potential. We refer the reader to Ref. 21 for the details of the definition of this system. The goal is to localize the wave packet at $x'=1.821$; this is expressed using $J_{1,\Delta T}$ via a target state ψ_{target} approximating a Dirac function centered in x_0 . The system is initially in the ground state. The time discretization method we have used is described in the Appendix.

Figure 2 represents the values of the tracking index during the control process as a function of the simulation time (each resolution of the time-dependent Schrödinger equation adds T to the simulation time). As predicted by the theory, a monotonic increase in the tracking index is observed.

This illustration speaks to the iterative character of the algorithms: even if it is usually understood that the monotonic algorithms are iterative, our findings, e.g., the availability at any intermediary times of a solution candidate and the interpretation as a local tracking trajectory procedure, support the view that the iterations are just a technical artifact due to the prescription of a time interval to control. Figure 2 graphically illustrates this interpretation. Because tracking algorithms usually deal with $[0, \infty]$ as time interval of control, we prove here that, on the one hand, the tracking approach can easily be adapted to a bounded interval of control

and, on the other hand, that the monotonic schemes can be “unfolded” to be read as a local tracking algorithm on $[0, +\infty]$.

B. Test of the stochastic monotonic algorithm

The stochastic monotonic algorithm in Sec. V was tested on a four-level system from the literature:¹⁶ the energy differences are $\epsilon_{31}=30$ and $\epsilon_{43}=\epsilon_{32}=20$ and the transition moment elements are $\mu_{31}=\mu_{32}=\mu_{43}$. The goal is to transfer the initial population from the lowest state $|1\rangle$ selectively to the second state $|2\rangle$. We employ a target operator $W=|2\rangle\langle 2|$.

Two monotonic algorithms have been compared: in a first test, the monotonic algorithms (23) and (24) have been used with the values $\delta=1.5$ and $\eta=0$. The value $\eta=0$ has been chosen for simplicity, while $\delta=1.5$ is the value in $[0,2]$ giving the best field after 15 iterations. In a second test, we kept $\eta=0$ and started from the same $\delta=1.5$ but we introduced a random change if $J_{\varepsilon, \tilde{\varepsilon}}^{fwd}(t_j) - J_{\varepsilon, \tilde{\varepsilon}}^{fwd}(t_{j-1}) < 10^{-10}$, where t_j is the j th time step and 10^{-10} is the typical value of $J_{\varepsilon, \tilde{\varepsilon}}^{fwd}(t_j) - J_{\varepsilon, \tilde{\varepsilon}}^{fwd}(t_{j-1})$ observed during the iterations of the first test.

The stochastic monotonic algorithm produces better fields of control than the fixed parameter monotonic algorithm. Figure 3 represents the values of the cost functional for the first 15 iterations of the two algorithms. In both cases, the target was reached accurately, the difference in converged functionals lies in the intensity of the control field, with the stochastic algorithm arriving always faster to the same functional quality.

VII. CONCLUSION

Starting from the need of intuitive understanding of the monotonic schemes, this paper documents the relation between these procedures and finite horizon local tracking algorithms. Despite the fact that all the presented algorithms are already available in the literature, this structural relationship has not, to the best of our knowledge, been documented. We show that local behavior exploits the availability, before the end of the current iteration, of the quality functional at the final time T . We introduce the necessary mathematical

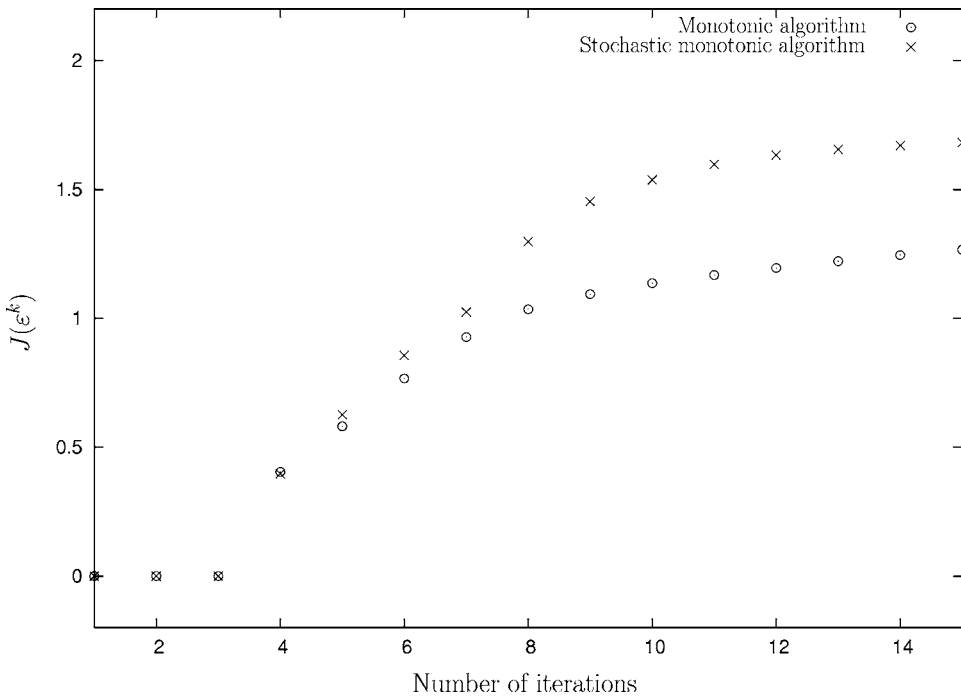


FIG. 3. Values of the cost functional during the 15 first iterations when using the algorithms (23) and (24) and the stochastic monotonic algorithm described in Sec. V. As $\varepsilon^0=0$ is a nonoptimal critical point, the initial field ε^0 was chosen as a sum of oscillations with frequencies ε_{31} and ε_{32} .

framework to support this interpretation and show that monotonicity is a natural consequence of the operating concepts. A proposal that exploits this information is the stochastic monotonic algorithm whose convergence properties are tested on a situation from the literature.

Furthermore, geometrical interpretation in terms of the distance between the system state and a related reference trajectory is also provided.

ACKNOWLEDGMENTS

One of the authors (G.T.) acknowledges support from INRIA Rocquencourt and CERMICS-ENPC.

APPENDIX: RELEVANT TIME DISCRETIZATIONS

In practice, we must choose an appropriate discrete propagation method to run these algorithms. Let us present it within the wave-function formulation. We use here a second-order potential centered split operator to solve numerically the propagation equations (41) and (39).

We consider two sequences $\varepsilon=(\varepsilon_j)_{j=0..N-1}$ and $\tilde{\varepsilon}=(\tilde{\varepsilon}_j)_{j=0..N-1}$ representing the time-discretized control fields and the corresponding discretized wave functions $\psi=(\psi_j)_{j=0..N}$, recursively computed by

$$\psi_{j+1}(x)=e^{-iH_0(\Delta T/2)}e^{i\mu\varepsilon_j\Delta T}e^{-iH_0(\Delta T/2)}\psi_j(x) \quad (\text{A1})$$

from a given initial condition ψ_0 . Consider also $\psi_{\text{ref}}=(\psi_{\text{ref},j})_{j=0..N}$ computed by

$$\psi_{\text{ref},j}(x)=e^{iH_0(\Delta T/2)}e^{-i\mu\tilde{\varepsilon}_j\Delta T}e^{iH_0(\Delta T/2)}\psi_{\text{ref},j+1}(x), \quad (\text{A2})$$

with the final condition $\psi_{\text{ref},N}=\psi_{\text{target}}$ or $\psi_{\text{ref},N}=O(\psi_N)$, according to the prescribed goal.

It is remarkable to notice that relevant discrete tracking index and quality functionals can lead to the same equivalence as before. We define a discrete forward quality functional by

$$J_{\Delta T, \varepsilon, \tilde{\varepsilon}}^{\text{fwd}}(n) = 2\Re\langle \psi_{\text{ref},n} | \psi_n \rangle - \alpha \Delta T \sum_{j=0}^{n-1} \varepsilon_j^2 - \alpha \Delta T \sum_{j=n}^{N-1} \tilde{\varepsilon}_j^2. \quad (\text{A3})$$

Let us also consider discrete quality functionals corresponding to (28) and (29) defined by

$$J_{1, \Delta T}(\varepsilon) = 2\Re\langle \psi_{\text{target}} | \psi_N \rangle - \alpha \Delta T \sum_{j=0}^{N-1} \varepsilon_j^2 \quad (\text{A4})$$

or

$$J_{2, \Delta T}(\varepsilon) = \langle \psi_N | O | \psi_N \rangle - \alpha \Delta T \sum_{j=0}^{N-1} \varepsilon_j^2. \quad (\text{A5})$$

The discrete derivative of the tracking index can be evaluated by

$$\begin{aligned} & J_{\Delta T, \varepsilon, \tilde{\varepsilon}}^{\text{fwd}}(n+1) - J_{\Delta T, \varepsilon, \tilde{\varepsilon}}^{\text{fwd}}(n) \\ &= 2\Re\langle \hat{\psi}_{\text{ref},n} | e^{i\mu(\varepsilon_n - \tilde{\varepsilon}_n)\Delta T} - Id | \hat{\psi}_n \rangle - \alpha \Delta T ((\varepsilon_n)^2 - (\tilde{\varepsilon}_n)^2) \\ &= -2\Re\langle \check{\psi}_{\text{ref},n+1} | e^{-i\mu(\varepsilon_n - \tilde{\varepsilon}_n)\Delta T} - Id | \check{\psi}_{n+1} \rangle \\ &\quad - \alpha \Delta T ((\varepsilon_n)^2 - (\tilde{\varepsilon}_n)^2), \end{aligned} \quad (\text{A6})$$

where we have used the following notations:

$$\hat{\psi}_m = e^{-iH_0(\Delta T/2)}\psi_m, \quad \check{\psi}_m = e^{iH_0(\Delta T/2)}\psi_m, \quad (\text{A7})$$

$$\hat{\psi}_{\text{ref},m} = e^{-iH_0(\Delta T/2)}\psi_{\text{ref},m}, \quad \check{\psi}_{\text{ref},m} = e^{iH_0(\Delta T/2)}\psi_{\text{ref},m}.$$

A simple computation leads to the discrete equivalent of (43) and (44),

$$\begin{aligned}
 & J_{1,\Delta T}(\varepsilon^{k+1}) - J_{1,\Delta T}(\varepsilon^k) \\
 &= \sum_{n=0}^{N-1} -J_{\Delta T, \varepsilon^k, \tilde{\varepsilon}^k}^{\text{fwd}}(n+1) + J_{\Delta T, \varepsilon^k, \tilde{\varepsilon}^k}^{\text{fwd}}(n) \\
 &\quad + \sum_{n=0}^{N-1} J_{\Delta T, \varepsilon^{k+1}, \tilde{\varepsilon}^k}^{\text{fwd}}(n+1) - J_{\Delta T, \varepsilon^{k+1}, \tilde{\varepsilon}^k}^{\text{fwd}}(n), \tag{A8} \\
 & J_{2,\Delta T}(\varepsilon^{k+1}) - J_{2,\Delta T}(\varepsilon^k) \\
 &= \langle \psi_N^{k+1} - \psi_N^k | O | \psi_N^{k+1} - \psi_N^k \rangle \\
 &\quad + \sum_{n=0}^{N-1} -J_{\Delta T, \varepsilon^k, \tilde{\varepsilon}^k}^{\text{fwd}}(n+1) + J_{\Delta T, \varepsilon^k, \tilde{\varepsilon}^k}^{\text{fwd}}(n) \\
 &\quad + \sum_{n=0}^{N-1} J_{\Delta T, \varepsilon^{k+1}, \tilde{\varepsilon}^k}^{\text{fwd}}(n+1) - J_{\Delta T, \varepsilon^{k+1}, \tilde{\varepsilon}^k}^{\text{fwd}}(n). \tag{A9}
 \end{aligned}$$

The computations of ε_n^k and $\tilde{\varepsilon}_n^k$ are then realized by a local maximization of (A6) with respect to these variables.

Remark 4. These formulas have been used to define monotonically discrete schemes in Refs. 26 and 27.

- ¹R. S. Judson and H. Rabitz, Phys. Rev. Lett. **68**, 1500 (1992).
- ²A. Assion, T. Baumert, M. Bergt, T. Brixner, B. Kiefer, V. Seyfried, M. Strehle, and G. Gerber, Science **282**, 919 (1998).
- ³M. Bergt, T. Brixner, B. Kiefer, M. Strehle, and G. Gerber, J. Phys. Chem. A **103**, 10381 (1999).
- ⁴T. C. Weinacht, J. Ahn, and P. H. Bucksbaum, Nature (London) **397**, 233 (1999).
- ⁵C. J. Bardeen, V. V. Yakovlev, K. R. Wilson, S. D. Carpenter, P. M. Weber, and W. S. Warren, Chem. Phys. Lett. **280**, 151 (1997).
- ⁶C. J. Bardeen, V. V. Yakovlev, J. A. Squier, and K. R. Wilson, J. Am.

- Chem. Soc. **120**, 13023 (1998).
- ⁷R. Kosloff, S. A. Rice, P. Gaspard, S. Tersigni, and D. J. Tannor, Chem. Phys. **139**, 201 (1989).
- ⁸P. Gross, H. Singh, H. Rabitz, K. Mease, and G. M. Huang, Phys. Rev. A **47**, 4593 (1993).
- ⁹Y. Chen, P. Gross, V. Ramakrishna, H. Rabitz, and K. Mease, J. Chem. Phys. **102**, 8001 (1995).
- ¹⁰W. Zhu and H. Rabitz, J. Chem. Phys. **119**, 3619 (2003).
- ¹¹M. Sugawara, J. Chem. Phys. **118**, 6784 (2003).
- ¹²M. Mirrahimi, G. Turinici, and P. Rouchon, J. Phys. Chem. A **109**, 2631 (2005).
- ¹³S. Shi, A. Woody, and H. Rabitz, J. Chem. Phys. **88**, 6870 (1988).
- ¹⁴T. Hornung, M. Motzkus, and R. de Vivie-Riedle, J. Chem. Phys. **115**, 3105 (2001).
- ¹⁵Y. Maday and G. Turinici, J. Chem. Phys. **118**, 8191 (2003).
- ¹⁶Y. Ohtsuki, G. Turinici, and H. Rabitz, J. Chem. Phys. **120**, 5509 (2004).
- ¹⁷Y. Maday, J. Salomon, and G. Turinici (unpublished).
- ¹⁸C. E. Garcia, D. M. Prett, and M. Morari, Automatica **25**, 335 (1989).
- ¹⁹J. B. Rawlings, E. S. Meadows, and K. R. Muske, Nonlinear Model Predictive Control: A Tutorial and Survey, ADCHEM '94 Proceedings, Kyoto, Japan, 1994.
- ²⁰J. B. Rawlings and K. R. Muske, IEEE Trans. Autom. Control **38**, 1512 (1993).
- ²¹W. Zhu and H. Rabitz, J. Chem. Phys. **109**, 385 (1998).
- ²²D. Tannor, V. Kazakov, and V. Orlov, *Time Dependent Quantum Molecular Dynamics*, edited by J. Broeckhove and L. Lathouwers (Plenum, New York, 1992), pp. 347–360.
- ²³S. Schirmer, M. Girardeau, and J. Leahy, Phys. Rev. A **61**, 012101 (2000).
- ²⁴Y. Ohtsuki, W. Zhu, and H. Rabitz, J. Chem. Phys. **110**, 9825 (1999).
- ²⁵G. Turinici, Monotonically Convergent Algorithms for Bounded Quantum Controls, Proceedings of the LHMNLCO3 IFAC Conference, 2003 (unpublished), pp. 263–266.
- ²⁶J. Salomon, Y. Maday, and G. Turinici, Discretely Monotonically Convergent Algorithm in Quantum Control, Proceedings of the LHMNLCO3 IFAC Conference, 2003, pp. 321–324.
- ²⁷Y. Maday, J. Salomon, and G. Turinici, Numer. Math. (in press).